Supporting Information

d- and *p*-block Single-atom Catalysts Supported by BN Nanocages toward electrochemical Reactions of N_2 and O_2

Chenhui Wang‡, Fan Huang‡, Haikuan Liang, Wei Nong†, Fei Tian*, Yan Li* and Chengxin Wang

State Key Laboratory of Optoelectronic Materials and Technologies, School of Materials Science and Engineering, Sun Yat-Sen (Zhongshan) University, Guangzhou 510275, People's Republic of China

* Corresponding Authors.

E-mail: tianf9@mail.sysu.edu.cn; liyan266@mail.sysu.edu.cn

‡ These authors contributed equally to this work.

†Wei Nong's present address: School of Materials Science and Engineering, Nanyang Technological University, 50 Nanyang Avenue, Singapore 639798, Singapore

Content

Note1. Supplementary computational details

The adsorption energy (E_{ads}) of the molecule (N_2, O_2 and H_2O) and atom (H, N, O and metals) on the substrate is calculated by

$$E_{\mathrm{ads}} = E_{\mathrm{total}} - E_{\mathrm{sub}} - E_{\mathrm{adsorbate}} \qquad \textbf{Eq.}\,1$$

where E_{total} is the total energy of the substrate with absorbed molecule or atom, E_{sub} is the total energy of the substrate, and $E_{\mathrm{adsorbate}}$ is the energy of adsorbate. In particular, the free energy of the O_2 gas molecule is determined by the equation[1]:

$$G_{\mathrm{O_2(g)}} = 4.92 - 2 \times G_{\mathrm{H_2O(l)}} - G_{\mathrm{H_2(g)}} \qquad \textbf{Eq.}\,2$$

in which $G(H_2O\ (l))$ can be calculated by carrying out calculation of $G(H_2O\ (g))$ at a pressure of 0.035 bar.

The cohesive energies are obtained from experimental data[2].

The Gibbs free energy (G) was obtained using the computational hydrogen electrode (CHE) model[3]. At the standard hydrogen electrode (SHE), the chemical potential of H^+/e^- pair in aqueous solution is equal to half that of hydrogen gas. According to the CHE model, the free energy change of reaction (ΔG) for each elementary step of NRR is expressed as

$$\Delta G = \Delta E - T\Delta S + \Delta ZPE - \Delta G_{\mathrm{U}} + \Delta G_{\mathrm{pH}} \qquad \textbf{Eq.}\,3$$

where ΔE is the change in total energies of the species involved in each step, ΔS and ΔZPE are the change in entropy and zero−point energies, respectively. Note that the entropies of gas molecules (N_2, H_2 and NH_3) are obtained from the NIST database[4], while those of the absorbed intermediates were set to zero. The zero-point energies of both gas molecules and intermediates were calculated using VASP and could be determined as $ZPE = ½\Sigma_i h\nu_i$, here h and ν_i are Planck constant and vibrational frequencies, respectively. T is the temperature and was set as 298.15 K here. $\Delta G_{\mathrm{U}} = neU$ is the free energy contributed by electrode potential, here n and U are the number of electrons transferred and the applied electrode potential, respectively. $\Delta G_{\mathrm{pH}} = k_{\mathrm{B}}T \times \ln 10 \times \mathrm{pH}$ is the correction of pH, here k_{B} is the Boltzmann constant, and pH = 0 was considered in this work.

The d band center, ε_d, was calculated as:

$$\varepsilon_d = \int_{-\infty}^{+\infty} \rho\varepsilon d\varepsilon \Big/ \int_{-\infty}^{+\infty} \varepsilon d\varepsilon \qquad \textbf{Eq.}\,4$$

where ρ and ε refer to the projected density of states (PDOS) of d orbital and energy level, respectively.

The limiting potential (LP) of the whole process is used to estimate the performance of NRR catalysts, which is determined by the potential determining step (PDS) that has the maximum ΔG values (ΔG_{PDS}) and by ΔG(*H) for NRR and HER, respectively, and can be calculated by

$$\mathrm{LP} = -\frac{\Delta G}{e} \qquad \textbf{Eq.}\,5$$

All the potential values are referenced to SHE.

We explored the 4e pathway of ORR and OER in an alkaline solution whose reactions are denoted as follows, in which * refers to the adsorption site.

The process of ORR:

$$\mathrm{O_2(g) + H_2O} + e^- + * \rightarrow * \mathrm{OOH + OH^-} \qquad \textbf{Eq.}\,6$$

$$* \mathrm{OOH} + e^- \rightarrow * \mathrm{O + OH^-} \qquad \textbf{Eq.}\,7$$

$$* \mathrm{O} + \mathrm{H_2O} + e^- \rightarrow * \mathrm{OH + OH^-} \qquad \textbf{Eq.}\,8$$

$$* \mathrm{OH} + e^- \rightarrow * + \mathrm{OH^-} \qquad \textbf{Eq.}\,9$$

and the process of OER:

$$* + \mathrm{OH^-} \rightarrow * \mathrm{OH} + e^- \qquad \textbf{Eq.}\,10$$

$$* \mathrm{OH + OH^-} \rightarrow * \mathrm{O + H_2O} + e^- \qquad \textbf{Eq.}\,11$$

$$* \mathrm{O + OH^-} \rightarrow * \mathrm{OOH} + e^- \qquad \textbf{Eq.}\,12$$

$$* \mathrm{OOH} + + \mathrm{OH^-} \rightarrow \mathrm{O_2(g) + H_2O} + e^- + * \qquad \textbf{Eq.}\,13$$

where * indicates the active center of the catalyst, (g) refers to the gas phase.

The adsorption free energy of intermediates during ORR/OER (*O_iH_i, i.e. *OOH, *O, *OH) are calculated by the following equation:

$$\Delta G_{*\mathrm{O}_i\mathrm{H}_j} = G_{*\mathrm{O}_i\mathrm{H}_j} - G_* - i \times G_\mathrm{O} - j/2 \times G_{*\mathrm{H_2}} \qquad \textbf{Eq.}\,14$$

where G_O was calculated according to the difference of $G(H_2O)$ and $G(H_2)$.

The Gibbs free energy change during ORR and OER can be obtained by the follows:

For ORR (Eq. 6-9):

$$\Delta G_1 = \Delta G_{*\mathrm{OOH}} - 4.92 \qquad \textbf{Eq.}\ 15$$

$$\Delta G_2 = \Delta G_{*\mathrm{O}} - \Delta G_{*\mathrm{OOH}} \qquad \textbf{Eq.}\ 16$$

$$\Delta G_3 = \Delta G_{*\mathrm{OH}} - \Delta G_{*\mathrm{O}} \qquad \textbf{Eq.}\ 17$$

$$\Delta G_4 = -\Delta G_{*\mathrm{OH}} \qquad \textbf{Eq.}\ 18$$

For OER (Eq. 10-13):

$$\Delta G_5 = \Delta G_{*\mathrm{OH}} \qquad \textbf{Eq.}\ 19$$

$$\Delta G_6 = \Delta G_{*\mathrm{O}} - \Delta G_{*\mathrm{OH}} \qquad \textbf{Eq.}\ 20$$

$$\Delta G_7 = \Delta G_{*\mathrm{OOH}} - \Delta G_{*\mathrm{O}} \qquad \textbf{Eq.}\ 21$$

$$\Delta G_8 = 4.92 - \Delta G_{*\mathrm{OOH}} \qquad \textbf{Eq.}\ 22$$

The overpotential η_{ORR} and η_{OER} are obtained by the following equations:

$$\eta_{\mathrm{ORR}} = 1.23 + \max(\Delta G_1, \Delta G_2, \Delta G_3, \Delta G_4) \qquad \textbf{Eq.}\ 23$$

$$\eta_{\mathrm{OER}} = \max(\Delta G_5, \Delta G_6, \Delta G_7, \Delta G_8) - 1.23 \qquad \textbf{Eq.}\ 24$$

Note2 Structure and features of TM@BNNC

Note2.1. Optimized configuration of the intermediates of the NRR distal pathway catalyzed by Os@BNNC and the N-N bond length of adsorbates.

Distal			
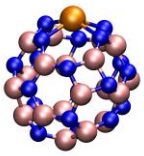	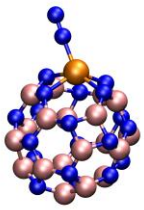	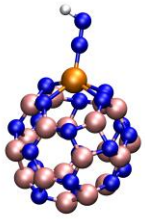	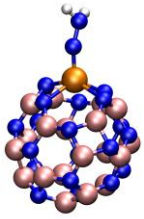
N/A	1.12 Å	1.21 Å	1.30 Å
*	*N	*NNH	*NNHH
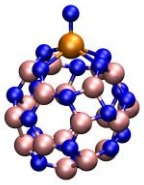	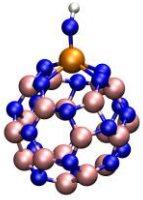	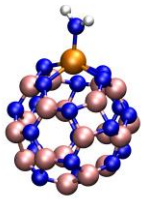	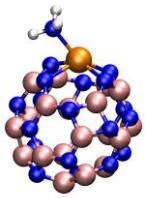
N/A	N/A	N/A	N/A
*N	*NH	*NH_2	*NH_3

Note2.2. Optimized configuration of the intermediates of the NRR alternating pathway catalyzed by Os@BNNC and the N-N bond length of adsorbates.

Alternating			
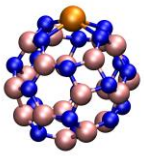	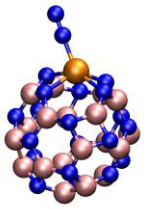	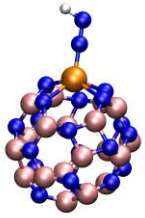	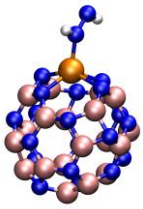
N/A	1.12 Å	1.21 Å	1.28 Å
*	*NN	*NNH	*NHNH
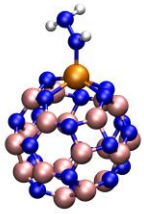	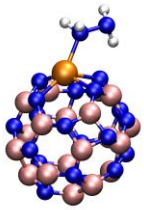	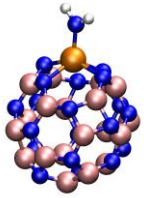	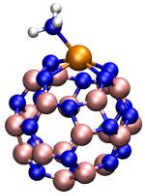
1.40 Å	1.46 Å	N/A	N/A
*NHNH	*NHHNHH	*NH_2	*NH_3

Note2.3. Optimized configuration of the intermediates of the NRR enzymatic pathway catalyzed by Os@BNNC and the N-N bond length of adsorbates.

Enzymatic			
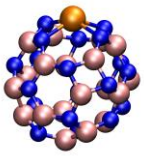	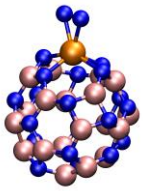	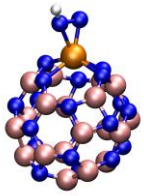	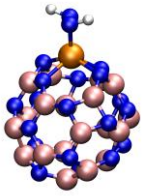
N/A	1.23 Å	1.28 Å	1.45 Å
*	**NN	**NNH	**NHNH
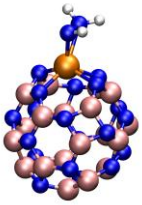	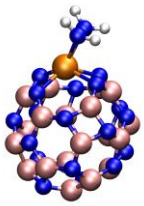	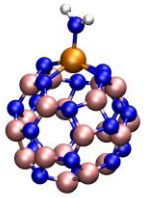	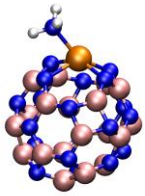
1.42 Å	1.44 Å	N/A	N/A
**NHNHH	**NHHNHH	*NH_2	*NH_3

Data1. For Section 3.1

Table S1. Adsorption energies (E_{ads}) of TM on BN nanocage, cohesive energies (E_{coh}) of the corresponding metal atom and the difference between them (E_{ads}−E_{coh}). The bold data refer to unstable TM@BNNCs. The unit is eV.

TM	E_{ads}	E_{coh}	$E_{ads} - E_{coh}$
Al	−7.34	−3.39	−3.95
Sc	–9.45	−3.90	−5.55
Ti	–10.71	−4.85	−5.86
V	–9.10	−5.31	−3.79
Cr	–6.85	−4.10	−2.75
Mn	–6.50	−2.92	−3.58
Fe	–7.02	−4.28	−2.74
Co	–6.30	−4.39	−1.91
Ni	–5.96	−4.44	−1.52
Cu	–3.90	−3.49	−0.41
Zn	–1.84	−1.35	−0.49
Y	–9.68	−4.37	−5.31
Zr	–12.35	−6.25	−6.10
Nb	–10.86	−7.57	−3.29
Mo	–8.56	−6.82	−1.74
Tc	–8.33	−6.85	−1.48
Ru	–7.87	−6.74	−1.13
Rh	–6.62	−5.75	−0.87
Pd	–3.94	−3.89	−0.05
Ag	–2.06	−2.95	**0.89**
Cd	–0.82	−1.16	**0.34**
Lu	–9.57	−4.43	−5.14
Hf	–12.45	−6.44	−6.01
Ta	–12.47	−8.10	−4.37
W	–12.17	−8.90	−3.27
Re	–10.53	−6.03	−4.50
Os	–8.50	−8.17	−0.33
Ir	–8.04	−6.94	−1.10
Pt	–6.08	−5.64	−0.44
Au	–3.09	−3.81	**0.72**
Hg	**0.22**	−0.67	**0.89**

Data2. For Section 3.2

Table S2. Adsorption energies (E_{ads}), *ZPE* and adsorption free energies (ΔG) during N_2 adsorption on TM@BNNCs. The unit is eV.

TM	E_{ads}	*ZPE*	ΔG	E_{ads}	*ZPE*	ΔG
Initial configuration	End-on(*NN)			Side-on(**NN)		
Sc	−0.41	0.17	0.20	−0.41	0.17	0.20
Ti	−0.65	0.19	−0.02	−0.64	0.19	−0.02
V	−0.60	0.19	0.03	−0.05	0.17	0.56
Cr	−0.36	0.19	0.27	0.31	0.18	0.92
Mn	−0.18	0.15	0.41	−0.22	0.18	0.39
Fe	−0.29	0.15	0.30	1.20	0.18	1.81
Co	0.00	0.23	0.67	−0.16	0.16	0.45
Ni	0.03	0.17	0.64	−0.07	0.16	0.53
Cu	−0.08	0.17	0.53	−0.06	0.17	0.54
Zn	−0.17	0.17	0.44	−0.17	0.16	0.44
Y	−0.33	0.18	0.29	−0.33	0.18	0.29
Zr	−0.56	0.18	0.06	−0.56	0.18	0.06
Nb	−0.68	0.19	−0.05	−0.48	0.19	0.15
Mo	−0.48	0.18	0.14	−0.26	0.20	0.38
Tc	−0.47	0.20	0.17	−0.21	0.20	0.42
Ru	−0.40	0.21	0.25	−0.12	0.20	0.52
Rh	−0.34	0.21	0.31	−0.05	0.16	0.54
Pd	−0.05	0.16	0.54	−0.07	0.16	0.53
Lu	−0.38	0.18	0.23	−0.38	0.17	0.23
Hf	−0.64	0.18	−0.02	−0.64	0.18	−0.02
Ta	−0.72	0.18	−0.10	−0.56	0.18	0.06
W	−0.77	0.18	−0.15	−0.75	0.20	−0.11
Re	−0.78	0.20	−0.14	−0.72	0.19	−0.10
Os	−0.55	0.21	0.10	−0.43	0.21	0.22
Ir	−0.48	0.22	0.18	−0.06	0.16	0.54
Pt	−0.14	0.21	0.51	−0.06	0.16	0.54

Table S3. Values of $\Delta G_{1\text{-}6}$ (eV) for NRR on TM@BNNCs (TM = Sc, Ti, V, Zr, Nb, Mo, Tc, Hf, Ta, W, Re, Os and Ir).

Element	ΔG_1	ΔG_1	ΔG_2	ΔG_2	ΔG_2	ΔG_6
Adsorption configuration	*NNH	**NNH	*NNHH	*NHNH	**NHNH	*NH_3
Sc	1.92	2.09	−0.21	−0.47	−0.49	−1.84
Ti	1.74	1.88	−0.17	−0.53	−0.43	−1.31
V	0.99		−0.26	−0.22		0.01
Zr	1.68		−0.10	−0.40		−1.12
Nb	0.63	0.34	−0.40	−0.10	−0.41	1.12
Mo	0.58		−0.66	−0.08		0.82
Tc	0.46		−0.75	0.24		0.56
Hf	1.59	1.68	−0.16	−0.42	−0.52	−1.03
Ta	0.42	0.08	−0.46	−0.10	−0.36	1.79
W	0.19	−0.10	−0.81	0.26	−0.52	1.25
Re	0.06	−0.25	−0.80	0.53	0.18	0.73
Os	0.27	0.73	−0.69	0.39	−0.18	0.29
Ir	0.61		−0.01	0.29		−0.37

Table S4. Gibbs free energy changes (eV) during the distal mechanism of NRR on TM@BNNCs (TM = Tc, Re, Os and Ir).

Step	Absorbate	TM = Tc	TM = Re	TM = Os	TM = Ir
0	$*N_2$	0.17	–0.14	0.10	0.18
1	*NNH	0.46	0.06	0.27	0.61
2	$*NNH_2$	–0.75	–0.80	–0.69	–0.01
3	*N	–0.16	–0.12	–0.63	–1.31
4	*NH	–0.72	–0.91	–0.33	0.85
5	$*NH_2$	–0.73	–0.30	–0.32	–1.22
6	$*NH_3$	0.56	0.73	0.29	–0.37
LP	/	–0.56	–0.73	–0.29	–0.85

Table S5. Gibbs free energy changes (eV) during the alternating mechanism of NRR on TM@BNNCs (TM = Tc, Re, Os and Ir).

Step	Absorbate	TM = Tc	TM = Re	TM = Os	TM = Ir
0	$*N_2$	0.17	–0.14	0.10	0.18
1	*NNH	0.46	0.06	0.27	0.61
2	*NHNH	0.24	0.53	0.39	0.29
3	*NHNHH	–0.84	–0.79	–0.69	–0.71
4	*NHHNHH	0.81	0.85	0.61	0.27
5	$*NH_2$	–2.57	–2.72	–2.27	–1.54
6	$*NH_3$	0.56	0.73	0.29	–0.37
LP	/	–0.81	–0.85	–0.61	–0.61

Table S6. Gibbs free energy changes (eV) during the enzymatic mechanism of NRR on TM@BNNCs (TM = Re and Os).

Step	Absorbate	TM = Re	TM = Os
0	$**N_2$	–0.10	0.22
1	**NNH	–0.25	0.73
2	**NHNH	0.18	–0.18
3	**NHNHH	–0.21	–0.40
4	**NHHNHH	0.81	0.36
5	$*NH_2$	–2.66	–2.33
6	$*NH_3$	0.73	0.29
LP	/	–0.81	–0.73

Table S7. Summary of SACs for NRR and their supports, single atom (SA), coordination and limiting potential (LP).

Supports	SA	Coordination	LP(V)	Reference
C_3N	Sc	MC_2N	–0.66	Refs.[5]
	Ti	MC_2N	–0.67	
	V	MC_2N	–0.63	
	Cr	MC_2N	–0.80	
	Mn	MC_2N	–0.75	
	Fe	MC_2N	–0.78	
	Co	MC_2N	–0.83	
	Ni	MC_2N	–0.75	
	Cu	MC_2N	–1.77	
	Zn	MC_2N	–1.40	
	Y	MC_2N	–0.73	
	Zr	MC_2N	–0.67	
	Nb	MC_2N	–0.97	
	Tc	MC_2N	–0.82	
	Ru	MC_2N	–0.94	
	Rh	MC_2N	–0.85	
	Pd	MC_2N	–0.66	
	Lu	MC_2N	–0.51	
	Hf	MC_2N	–0.84	
	Ta	MC_2N	–1.27	
	Re	MC_2N	–1.16	
	Ir	MC_2N	–0.74	
	Pt	MC_2N	–0.74	
	Sc	MC_3	–0.84	
	Ti	MC_3	–0.93	
	V	MC_3	–0.59	
	Cr	MC_3	–0.80	
	Mn	MC_3	–0.65	
	Fe	MC_3	–0.89	
	Co	MC_3	–1.19	
	Ni	MC_3	–0.98	
	Zn	MC_3	–1.32	
	Y	MC_3	–1.00	
	Zr	MC_3	–1.03	
	Nb	MC_3	–0.78	

Tc	MC_3	–0.60	Refs.[5]
Ru	MC_3	–1.39	
Rh	MC_3	–1.46	
Pd	MC_3	–0.95	
Lu	MC_3	–0.94	
Hf	MC_3	–1.17	
Ta	MC_3	–0.70	
Re	MC_3	–0.86	
Ir	MC_3	–1.16	
Pt	MC_3	–0.74	
Sc	MC_4	–1.13	
Ti	MC_4	–0.66	
V	MC_4	–0.73	
Cr	MC_4	–0.45	
Mn	MC_4	–0.47	
Fe	MC_4	–0.75	
Co	MC_4	–1.17	
Ni	MC_4	–2.01	
Cu	MC_4	–2.30	
Zn	MC_4	–1.21	
Y	MC_4	–1.20	
Zr	MC_4	–0.68	
Nb	MC_4	–0.89	
Mo	MC_4	–0.92	
Tc	MC_4	–0.67	
Ru	MC_4	–0.83	
Rh	MC_4	–1.17	
Pd	MC_4	–2.07	
Ag	MC_4	–2.24	
Lu	MC_4	–1.07	
Hf	MC_4	–0.75	
Ta	MC_4	–1.28	
W	MC_4	–1.27	
Re	MC_4	–3.07	
Os	MC_4	–0.54	
Ir	MC_4	–0.96	
Pt	MC_4	–1.98	
Au	MC_4	–2.21	

	Hg	MC_4	–2.17	Refs.[5]
	Sc	MC_2N_2	–0.77	
	Ti	MC_2N_2	–0.84	
	V	MC_2N_2	–0.62	
	Cr	MC_2N_2	–0.40	
	Mn	MC_2N_2	–0.79	
	Fe	MC_2N_2	–0.62	
	Co	MC_2N_2	–1.04	
	Ni	MC_2N_2	–2.30	
	Cu	MC_2N_2	–2.31	
	Zn	MC_2N_2	–1.85	
	Y	MC_2N_2	–0.88	
	Zr	MC_2N_2	–0.95	
	Nb	MC_2N_2	–0.81	
	Mo	MC_2N_2	–0.80	
	Tc	MC_2N_2	–0.65	
	Ru	MC_2N_2	–1.01	
	Rh	MC_2N_2	–0.87	
	Pd	MC_2N_2	–2.48	
	Ag	MC_2N_2	–2.25	
	Cd	MC_2N_2	–1.63	
	Lu	MC_2N_2	–0.76	
	Hf	MC_2N_2	–1.14	
	Ta	MC_2N_2	–1.14	
	W	MC_2N_2	–1.05	
	Re	MC_2N_2	–1.01	
	Os	MC_2N_2	–0.55	
	Ir	MC_2N_2	–0.79	
	Pt	MC_2N_2	–2.43	
	Au	MC_2N_2	–2.18	
	Hg	MC_2N_2	–1.32	
Graphene	Mo	MC_3	–0.89	Refs.[6]
	Nb	MC_3	–0.83	
	V	MC_3	–0.99	
	W	MC_3	–0.75	
	Ir	MC_4	–0.66	
	Co	MC_4	–1.00	
	Ir	MC_4	–0.79	

	Mo	MC_4	–0.69	Refs.[6]
	Nb	MC_4	–0.61	
	Os	MC_4	–0.69	
	V	MC_4	–0.70	
	Ta	MC_4	–0.92	
	Re	MC_4	–0.60	
	La	MN_3	–0.70	
	Mn	MN_3	–1.00	
	Sc	MN_3	–0.89	
	Ti	MN_3	–0.77	
	Y	MN_3	–0.97	
	V	MN_4	–0.87	
	Cr	MN_4	–0.98	
	Sc	MN_4	–0.81	
	Y	MN_4	–0.97	
	Ti	MN_4	–0.69	
Graphene oxide	Pt	cluster	–0.68	Refs.[7]
	Cu	cluster	–1.52	
	Co	cluster	–1.24	
	Ni	cluster	–1.52	
Graphene	Fe	MN_3	–0.66	Refs.[8]
	Fe	MC_3	–1.37	
	Fe	MC_2N	–1.16	
	Fe	MCN_2	–0.80	
	Fe	MP_3	–0.92	
C_2N	Ru	MN_2	–0.96	Refs.[9]
γ-graphyne	Ru	MC_6	–0.98	
t-C_3N_4	Ru	MN_3	–0.94	
g-C_3N_4	V	MC_2N_3	–0.53	Refs.[10]
(corrugated+ N)	Ti	MCN_2	–0.51	
Graphene	Mo	MC_2N	–0.40	Refs.[11]
C_2N	Mo	MN_2	–0.17	Refs.[12]
	Ti	MN_2	–0.45	
	V	MN_2	–0.55	
	Ni	MN_2	–0.79	
Graphene	Nb	MC_3	–0.45	Refs.[13]
	Re	MC_3	–0.43	

	V	MC_2N	–0.52	Refs.[13]
	Nb	MC_2N	–0.41	
	Mo	MC_2N	–0.40	
	V	MN_4	–0.41	
	Ru	MC_2N	–0.60	
	V	MCN_3	–0.35	
	W	MC_3	–0.25	
	Zr	MC_2N	–0.55	
	Fe	MN_4	–1.38	Refs.[14]
	Co	MN_4	–1.09	
	Ru	MN_4	–1.27	
	Rh	MN_4	–1.23	
	Mo	MN_4	–0.67	
	W	MN_4	–1.08	
g-C_3N_4	Pt	MN_4	–0.24	Refs.[15]
	W	MN_2	–0.35	Refs.[16]
	V	MN_6	–0.52	Refs.[17]
	Cr	MN_6	–1.23	
	Mn	MN_6	–1.23	
	Fe	MN_6	–0.81	
	Ag	MN_6	–2.20	
	Au	MN_6	–0.94	
	Ru	MN_6	–0.33	
	Rh	MN_6	–0.45	
	Co	MN_6	–0.61	
	Ni	MN_6	–1.15	
	Cu	MN_6	–1.79	
	Pd	MN_6	–1.13	
	Nb	MN_6	–0.53	
	Mo	MN_6	–0.62	
	Tc	MN_6	–0.43	
	Ta	MN_6	–1.00	
	W	MN_6	–0.65	
	Re	MN_6	–0.83	
	Ir	MN_6	–0.98	
	Pt	MN_6	–0.98	
α-Boron sheet	Ru	MB_6	–0.42	Refs.[18]
β12-Boron sheet	Ru	MB_6	–0.44	

C_2N	Cr	MN_2	–1.69	Refs.[19]
	Mn	MN_2	–0.69	
	Fe	MN_2	–1.06	
	Co	MN_2	–1.02	
	Ni	MN_2	–1.22	
	Cr	M_2N_4	–0.34	
	Co	M_2N_4	–0.54	
	Ni	M_2N_4	–0.42	
	Mn	M_2N_4	–0.23	
	Fe	M_2N_4	–0.24	
	Mo	M_2N_6	–0.41	Refs.[20]
	Fe	M_2N_6	–1.23	
MoS_2	Fe	M	–1.02	Refs.[21]
	AuCu	MO_x	–1.82	Refs.[22]
Black phosphorus	B	MP_3	–0.58	Refs.[23]
	B	M_2P_6	–0.19	
MoS_2	Mo	MoS_3	–0.44	Refs.[24]
C_2N	B	BN_2	–0.25	Refs.[25]
Graphene	Ru	MN_3	–0.73	Refs.[26]
$LiFeO_2$(111)	Fe	M	–0.63	Refs.[27]
BO-MnO_2(VO)	Mn	M	–0.83	Refs.[28]
BS-VS_2(VS)	V	M	–0.77	Refs.[29]
Fe-CeO_2(VO)	Ce	M	–0.81	Refs.[30]
MoSn-SnS_2(VS)	MoSn	M	–0.73	Refs.[31]
GDY(graphdiyne	B	/	–0.77	Refs.[32]
GDY	BN	/	–0.48	
CN	Fe2	/	–0.47	Refs.[33]
	Co	/	–0.87	
h-BN	Mo	MN_3	–0.35	Refs.[34]
ZIF-8 precursor graphene	Ni	/	–0.79	Refs.[35]
	FeMo	/	–1.79	
GY(graphyne)	Mn	/	–0.36	Refs.[36]
MnO_2	none	/	–1.59	Refs.[28]
	B	/	–0.83	
Re_2MnS_6	Ultrathin nanosheets		–0.51	Refs.[37]

Data3. For Section 3.4

Table S8. *d*-band centers (ε_d) of TM@BNNCs. The unit is eV.

TM	d-total	d*xy*	d*yz*	dx^2	d*xz*	dz^2
Sc	2.94	0.46	2.87	3.59	3.08	3.34
Ti	0.62	0.69	0.35	0.87	0.50	0.66
V	0.09	0.02	0.07	0.05	0.09	0.25
Cr	–0.01	0.21	–0.28	0.13	–0.07	–0.07
Mn	–0.41	–0.26	–0.48	–0.44	–0.48	–0.42
Fe	–1.78	–1.72	–1.88	–1.87	–1.75	–1.67
Co	–1.38	–1.25	–1.28	–1.52	–1.43	–1.43
Ni	–1.67	–1.66	–1.65	–1.97	–1.51	–1.58
Cu	–2.45	–2.54	–2.36	–2.85	–2.33	–2.17
Zn	–6.11	–5.89	–6.23	–6.22	–6.19	–6.04
Y	2.99	–1.34	2.40	4.16	3.01	3.91
Zr	0.49	–2.66	0.28	1.41	0.59	1.21
Nb	–0.44	–2.66	–0.37	–0.01	–0.19	0.19
Mo	–0.81	–1.62	–1.06	–0.35	–0.73	–0.47
Tc	–1.39	–1.39	–1.65	–1.29	–1.40	–1.23
Ru	–1.25	–0.91	–1.58	–1.23	–1.30	–1.22
Rh	–1.75	–1.50	–1.91	–1.86	–1.78	–1.69
Pd	–2.26	–2.21	–2.25	–2.54	–2.25	–2.06
Lu	2.79	–2.32	2.24	4.48	3.01	3.66
Hf	0.67	–3.86	0.39	1.96	0.81	1.61
Ta	–0.68	–4.54	–0.61	0.07	–0.24	0.20
W	–0.90	–3.41	–0.91	–0.17	–0.63	–0.35
Re	–1.73	–3.60	–1.74	–1.22	–1.40	–1.21
Os	–1.96	–2.80	–2.11	–1.41	–1.96	–1.70
Ir	–2.12	–2.35	–2.20	–2.15	–1.93	–1.94
Pt	–2.49	–2.54	–2.54	–2.77	–2.36	–2.24

Table S9. Global magnetic moment of TM@BNNCs with the local magnetic moment of TM. The unit is μ_B/Å^3.

Element	TM@BNNC	TM	Element	TM@BNNC	TM
Sc	0.81	0.01	Ru	0.26	0.05
Ti	0.00	0.00	Rh	1.00	0.59
V	1.00	0.94	Pd	0.02	0.02
Cr	2.00	2.20	Lu	0.78	0.03
Mn	3.08	3.20	Hf	0.00	0.00
Fe	3.92	3.06	Ta	1.00	0.54
Co	2.90	1.82	W	1.99	1.53
Ni	1.93	0.81	Re	3.00	2.30
Cu	0.89	0.06	Os	2.09	1.44
Zn	0.67	0.03	Ir	1.00	0.63
Y	0.81	0.01	Pt	0.00	0.00
Zr	0.00	0.00			
Nb	1.00	0.59			
Mo	2.00	1.65			
Tc	3.00	2.34			

Table S10. Adsorption energies (eV) of O_2 and H_2O on TM@BNNCs.

TM	E_{ads}(*O_2)	E_{ads}(*H_2O)	TM	E_{ads}(*O_2)	E_{ads}(*H_2O)
Sc	–0.61	–1.08	Ru	–1.63	–0.66
Ti	–1.37	–1.40	Rh	–0.81	–0.68
V	–2.41	–1.15	Pd	–0.28	–0.40
Cr	–2.02	–1.88	Lu	–0.74	–1.05
Mn	–0.90	–1.34	Hf	–1.62	–1.43
Fe	–0.60	–0.76	Ta	–3.33	–0.83
Co	–0.61	–0.70	W	–4.59	–0.87
Ni	–0.23	–0.41	Re	–3.68	–0.82
Cu	–0.06	–0.31	Os	–2.27	–0.60
Zn	–0.11	–0.64	Ir	–0.81	–0.63
Y	–0.65	–0.93	Pt	–0.29	–0.48
Zr	–1.37	–1.28			
Nb	–3.08	–0.79			
Mo	–3.62	–0.88			
Tc	–2.87	–0.62			

Table S11. Adsorption Gibbs free energies (eV) of reaction intermediates of OOH, O and OH and overpotentials for ORR/OER on TM@BNNCs. The bold data refer to TM@BNNCs with competitive catalytic performance for ORR/OER.

ORR-OER					
TM	ΔG*OOH	ΔG *O	ΔG *OH	η_{ORR}	η_{OER}
Sc	3.99	3.51	0.64	**0.75**	1.64
Ti	3.05	1.85	–0.41	1.64	1.03
V	2.20	–0.20	–1.31	2.54	1.49
Cr	2.72	–0.05	–0.76	1.99	1.54
Mn	3.53	0.58	0.16	1.07	1.72
Fe	3.81	1.24	0.77	0.76	1.34
Co	3.67	2.07	0.91	0.32	**0.37**
Ni	4.63	3.33	1.55	0.94	**0.55**
Cu	5.20	1.81	2.53	1.95	2.16
Zn	4.88	0.96	1.68	1.95	2.69
Y	3.99	3.58	0.65	0.82	1.70
Zr	2.96	2.09	–0.51	1.74	1.37
Nb	1.36	–0.71	–2.14	3.37	2.33
Mo	0.16	–1.48	–1.71	2.94	3.53
Tc	0.49	–1.48	–1.19	2.42	3.20
Ru	2.08	–0.86	–0.44	1.67	1.71
Rh	3.54	1.25	0.35	0.88	1.06
Pd	4.49	3.24	1.50	0.80	**0.51**
Lu	3.89	3.50	0.52	0.84	1.75
Hf	2.72	1.94	–0.80	2.03	1.51
Ta	1.09	–0.82	–2.48	3.71	2.60
W	–0.83	–2.41	–2.21	3.44	4.52
Re	–0.86	–2.30	–1.62	2.85	4.55
Os	0.91	–1.57	–0.70	2.10	2.78
Ir	3.10	0.61	0.04	1.19	1.26
Pt	4.29	2.82	1.20	**0.60**	**0.39**

Table S12. Summary of Bifunctional catalysts, their supports and overpotentials (V).

CATALYSTS	Supports or Comments	η_{ORR}	η_{OER}	Refs.
Au	C_2N	0.38	0.79	Refs.[38]
Pd		0.40	0.71	
Cu		0.51	0.71	
Rh		0.67	0.37	
Ni		0.71	0.55	
Cd		0.81	1.54	
Ag		1.08	1.12	
Pt		1.14	0.40	
Ir		1.14	0.60	
Co		1.17	0.71	
Ru		1.24	0.92	
Fe		1.41	0.83	
Cr		1.45	1.85	
Os		1.46	1.09	
Zn		1.71	1.53	
Mn		1.81	1.56	
Mo		1.92	4.56	
V		2.09	3.61	
La		2.39	1.58	
Ta		2.62	5.99	
Nb		2.76	5.55	
Ti		2.84	4.52	
Y		2.85	2.02	
Sc		2.94	1.92	
Zr		3.13	4.86	
Hf		3.41	5.05	
W		3.47	6.01	
IrN_4	G	0.26	0.30	Refs.[39]
Ir	pyrrolic-N_4-G	0.34	0.32	Refs.[40]
Co-Ag	MN_4-O-MN_4	0.35	0.33	Refs.[41]
Co-Cu		0.35	0.38	
Fe-Cu		0.36	0.41	
Co-Ni		0.43	0.42	
A-1	N-doped graphene nanoribbon	0.45	0.91	Refs.[42]
A-3		0.55	0.50	
Ad-1		1.09	1.72	
A-2		0.63	0.74	
Zd-2		0.63	1.21	
At-3		1.34	2.00	
Z-1		0.67	1.24	

Ad-2	N-doped graphene nanoribbon	0.77	1.07	Refs.[42]
Ad-3		0.77	1.42	
Z-2		0.85	0.95	
At-1		0.87	1.48	
At-4		0.87	1.49	
Z-3		0.88	0.96	
Zd-1		1.30	2.02	
2gN-1	N-doped graphene nanosheet	0.60	1.02	
1gN-1		0.65	0.67	
PC		1.03	1.08	
1pdN-1		1.17	1.09	
1prN-2		1.30	0.95	
3gN-1		1.39	2.08	
CoN1	N-doped graphene	0.94	1.68	Refs.[43]
CoN_2-opp		1.10	1.81	
CoN_2-pen		0.98	1.69	
CoN_2-hex		0.61	1.36	
CoN_3		0.63	1.36	
CoN_4		0.47	0.69	
CoN_1	N-doped graphene	1.08	0.90	Refs.[44]
CoN_2		0.69	0.63	
CoN_3		0.53	0.73	
CoN_4		0.30	0.41	
Ni-$Mo_2B_2O_2$	MXenes	0.23	0.54	Refs.[45]
(001)	V_4C_3	0.89	1.56	Refs.[46]
(110)		3.98	6.51	
(111)		2.84	6.68	
(001)	VC	1.11	1.91	
(110)		2.72	5.16	
(111)		4.11	7.66	
(001)	V_8C_7	0.91	1.55	
(110)		2.39	5.68	
(111)		2.17	2.55	
Pure	M-cementite	0.89	1.52	Refs.[47]
Co dope at Fe1		0.85	1.55	
Co dope at Fe2		0.85	1.46	
Co dope at Fe3		0.88	1.50	
Co dope at Fe4		0.87	1.50	
Co dope at Fe		0.68	1.12	
Mn dope at Fe1		1.09	1.93	
Ni dope at Fe1		0.64	0.78	
TiC_2	MC_2	0.66	0.95	Refs.[48]
VC_2		0.78	0.68	

NbC_2	MC_2	0.66	0.93	Refs.[48]
TaC_2		0.37	0.72	
MoC_2		0.47	0.45	
$Ni_{1.5}Co_{1.5}N$	$PF/Ni_{1.5}Co_{1.5}N$	1.18	1.81	Refs.[49]
$PF/Ni_{1.5}Co_{1.5}N$		0.68	1.02	
Nb_2CO_2	Nb_2CT_2	1.04	0.94	Refs.[50]
Nb_2CF_2		1.01	1.57	
Nb_2CO_2–Pd		0.90	0.56	
Nb_2CO_2–Pt		0.72	1.11	
Nb_2CF_2–Pd		0.78	0.45	
Nb_2CF_2–Pt		0.71	0.52	
Nb_2CO_2–VO–Pd		0.51	0.46	
Nb_2CO_2–VO–Pt		0.47	0.39	
Nb_2CF_2–VF–Pd		0.47	0.88	
Nb_2CF_2–VF–Pt		0.40	0.37	
Sc	pyridine-4N	3.52	2.50	Refs.[51]
Ti		2.79	2.10	
V		2.38	1.64	
Cr		1.20	1.89	
Mn		1.08	1.49	
Fe		0.42	0.72	
Co		0.50	0.37	
Ni		0.60	0.33	
Cu		0.57	0.48	
Zn		1.33	0.84	
Y		3.30	2.46	
Zr		2.52	1.94	
Nb		2.09	2.16	
Mo		1.23	1.78	
Tc		0.97	1.49	
Ru		0.89	0.45	
Rh		0.77	0.36	
Pd		1.64	1.31	
Ag		0.75	0.55	
Cd		1.30	0.66	
Hf		2.73	2.05	
Ta		2.42	1.72	
W		1.75	2.36	
Re		1.50	2.25	
Os		0.68	1.16	
Ir		0.94	0.37	
Pt		1.41	1.21	
Au		2.13	1.99	
Sc	pyrrole-4N	3.36	2.44	

Ti	pyrrole-4N	2.72	1.80	Refs.[51]
V		2.25	1.71	
Cr		0.80	1.22	
Mn		0.59	1.20	
Fe		0.45	0.86	
Co		0.60	0.32	
Ni		1.47	0.85	
Cu		2.01	1.49	
Zn		2.18	1.45	
Y		3.57	2.81	
Zr		2.76	2.01	
Nb		1.66	2.28	
Mo		0.65	0.96	
Tc		0.40	1.13	
Ru		0.91	0.41	
Rh		1.69	0.91	
Pd		2.52	1.89	
Ag		2.55	1.82	
Cd		2.43	1.77	
Hf		2.87	2.18	
Ta		2.39	1.57	
W		1.40	2.29	
Re		0.68	0.88	
Os		0.47	0.62	
Ir		0.60	0.29	
Pt		1.67	0.94	
Au		2.83	2.11	

Supplementary Figures

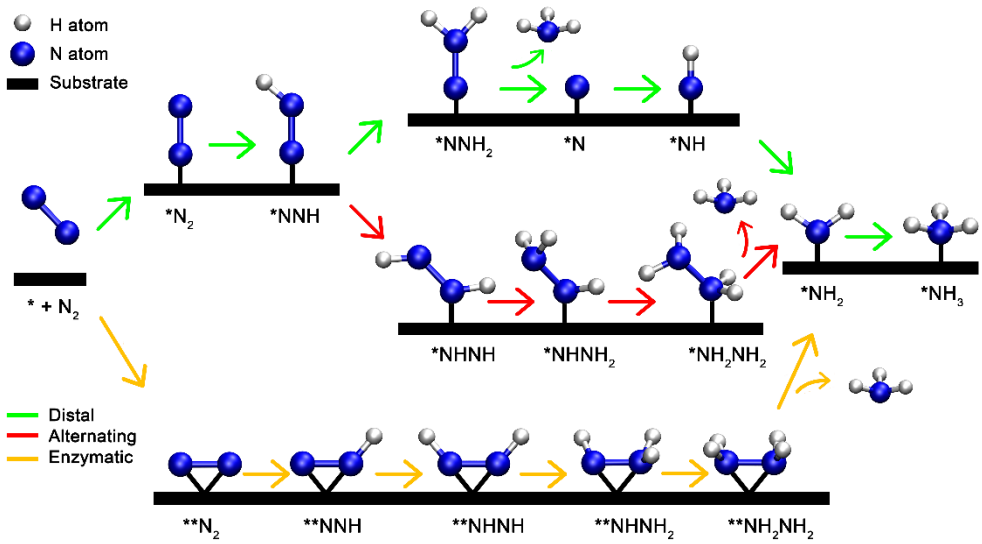

Fig. S1. Schematic depiction of possible reaction pathways of NRR. Imaginary atomic configurations of involved intermediates are illustrated. * means adsorption site. ** + intermediate (N_2, NNH, NHNH, etc.) and * + intermediate are for side-on and end-on adsorption nitrogen fixed pathway respectively. Besides, the first N in *NN means proximal nitrogen atom, and the second N means distal one.

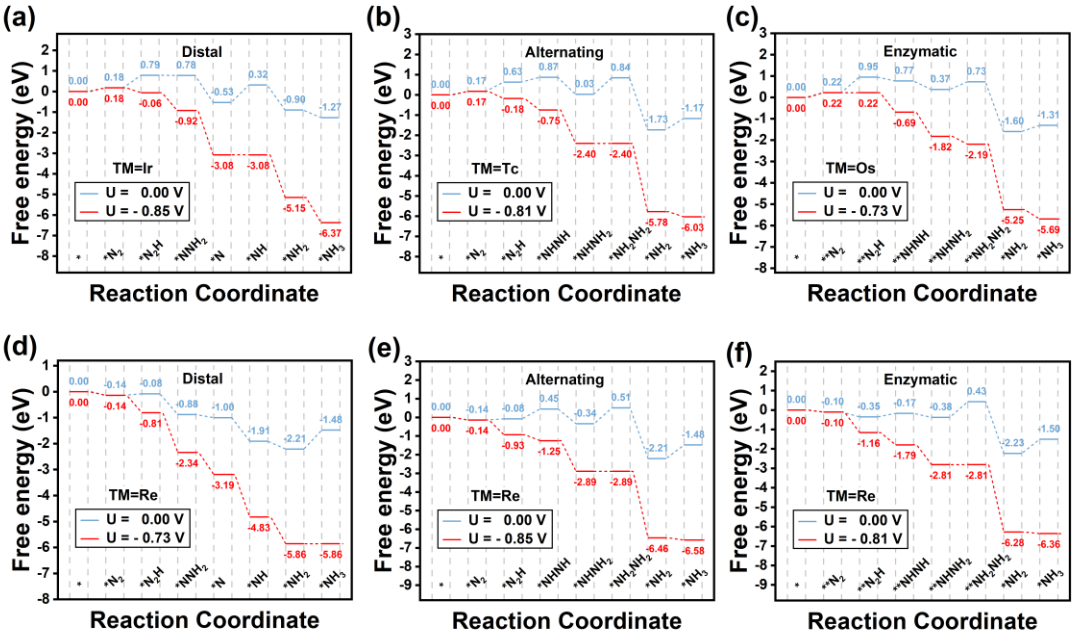

Fig. S2. Free-energy diagrams through various mechanisms for NRR on (a) Ir@BNNC, (b) Tc@BNNC, (c) Os@BNNC and (d-f) Re@BNNC at zero and applied potentials, respectively.

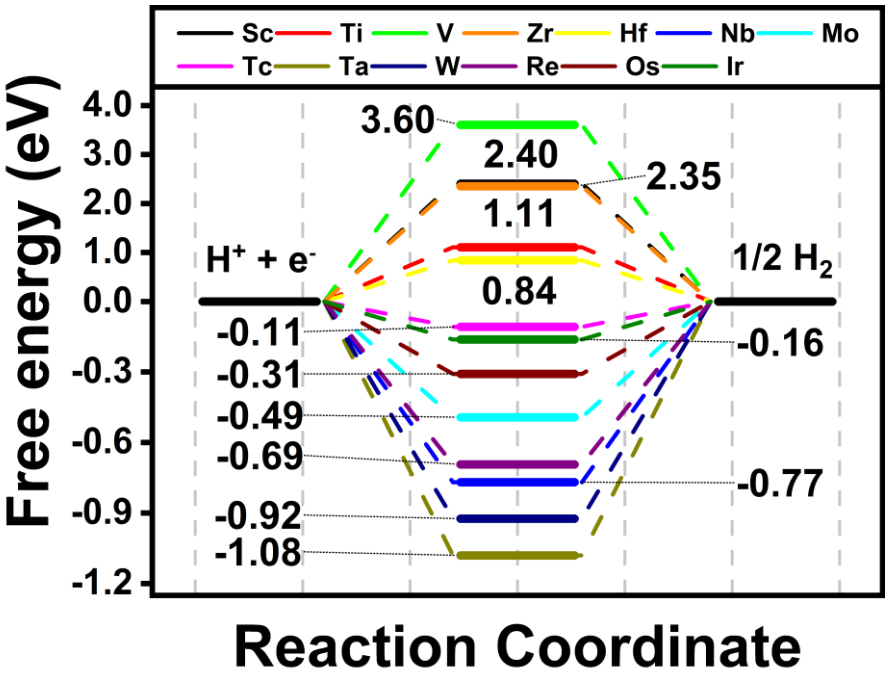

Fig. S3. The free energy changes of HER on TM@BNNCs that pass the screening.

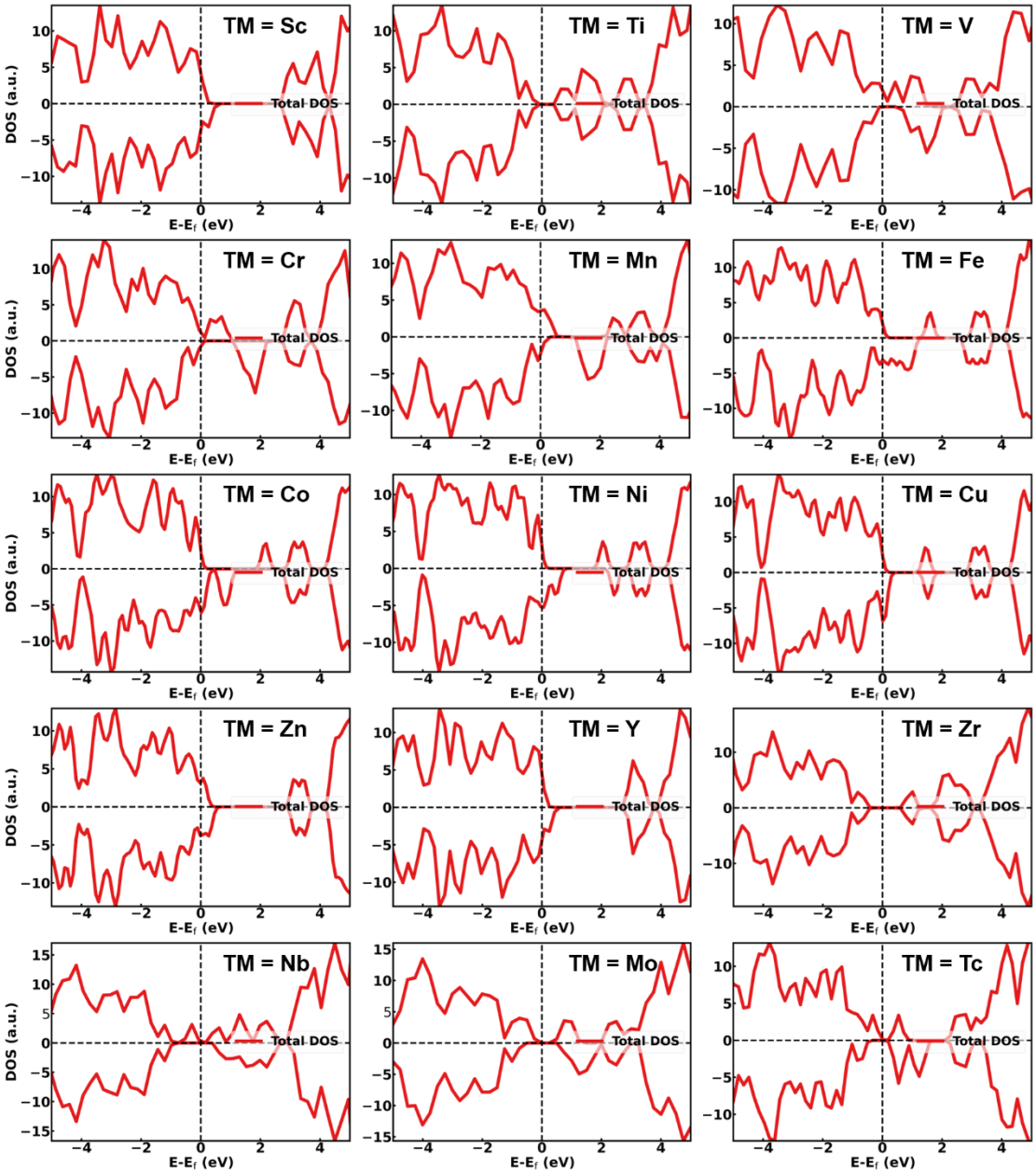

Fig. S4. Density of states (DOS) of TM@BNNCs (TM = Sc, Ti, V, Cr, Mn, Fe, Co, Ni, Cu, Zn, Y, Zr, Nb, Mo and Tc).

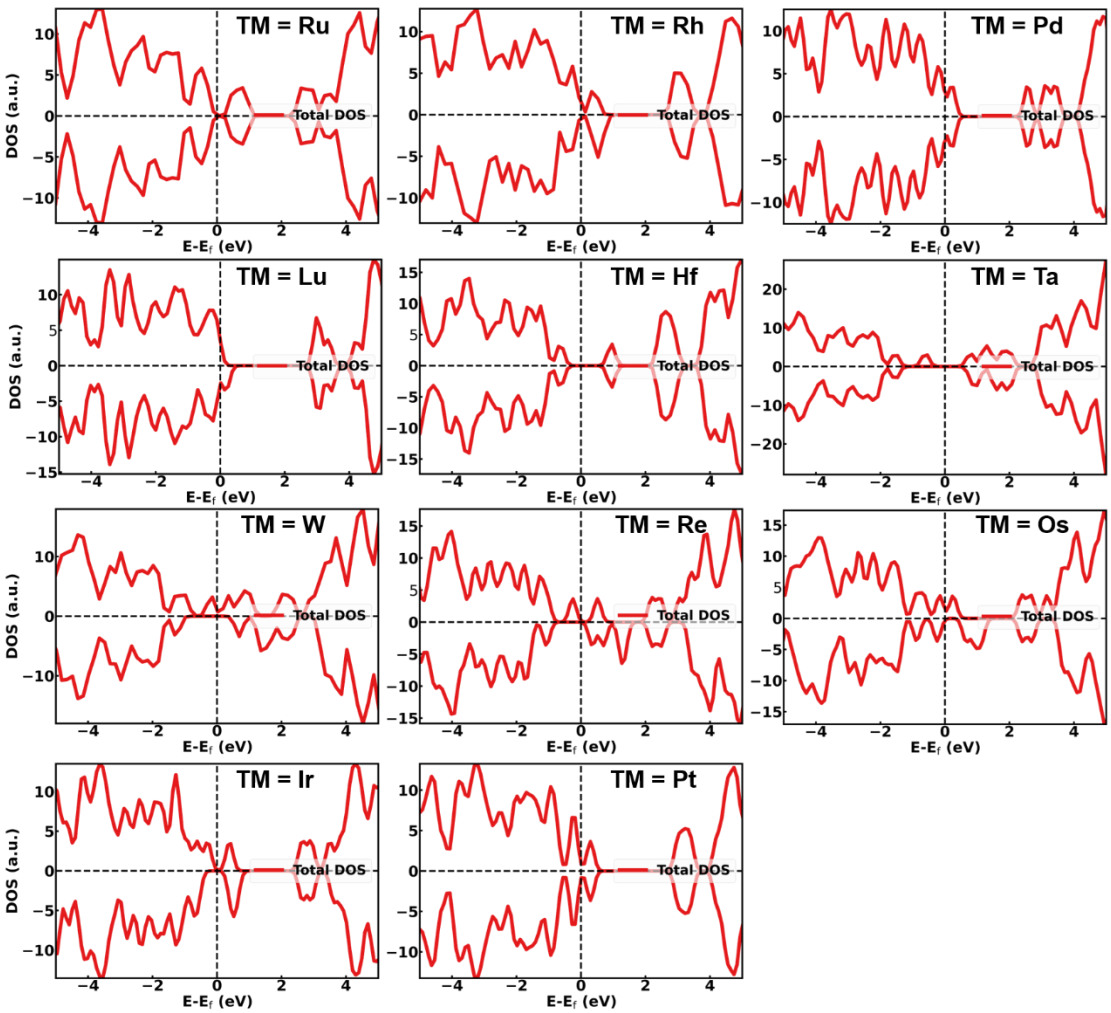

Fig. S5. Density of states (DOS) of TM@BNNCs (TM = Ru, Rh, Pd, Lu, Hf, Ta, W, Re, Os, Ir, and Pt).

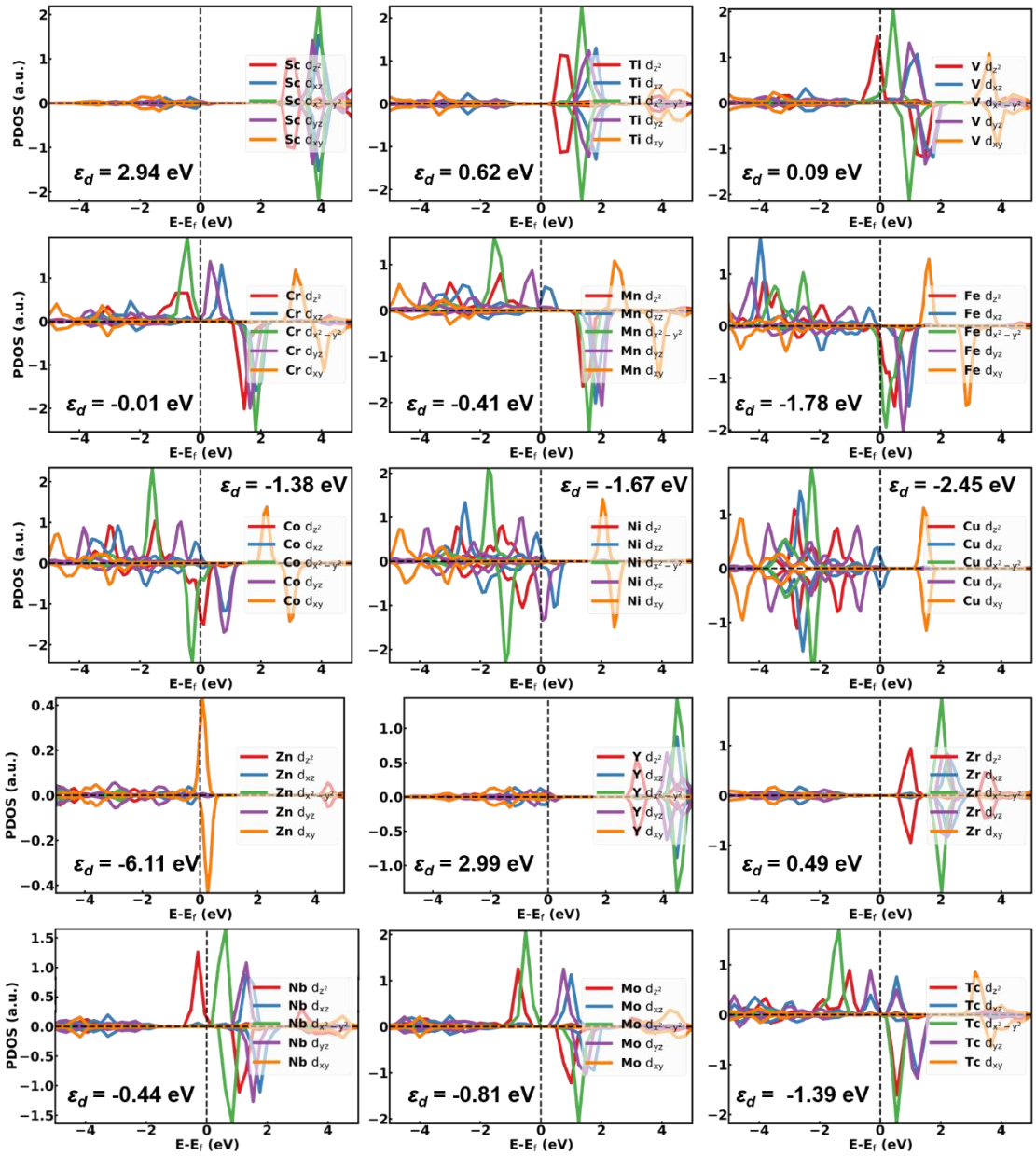

Fig. S6. Projected density of states (PDOS) of *d* orbitals and corresponding *d*-band centers for TM@BNNCs (TM = Sc, Ti, V, Cr, Mn, Fe, Co, Ni, Cu, Zn, Y, Zr, Nb, Mo and Tc).

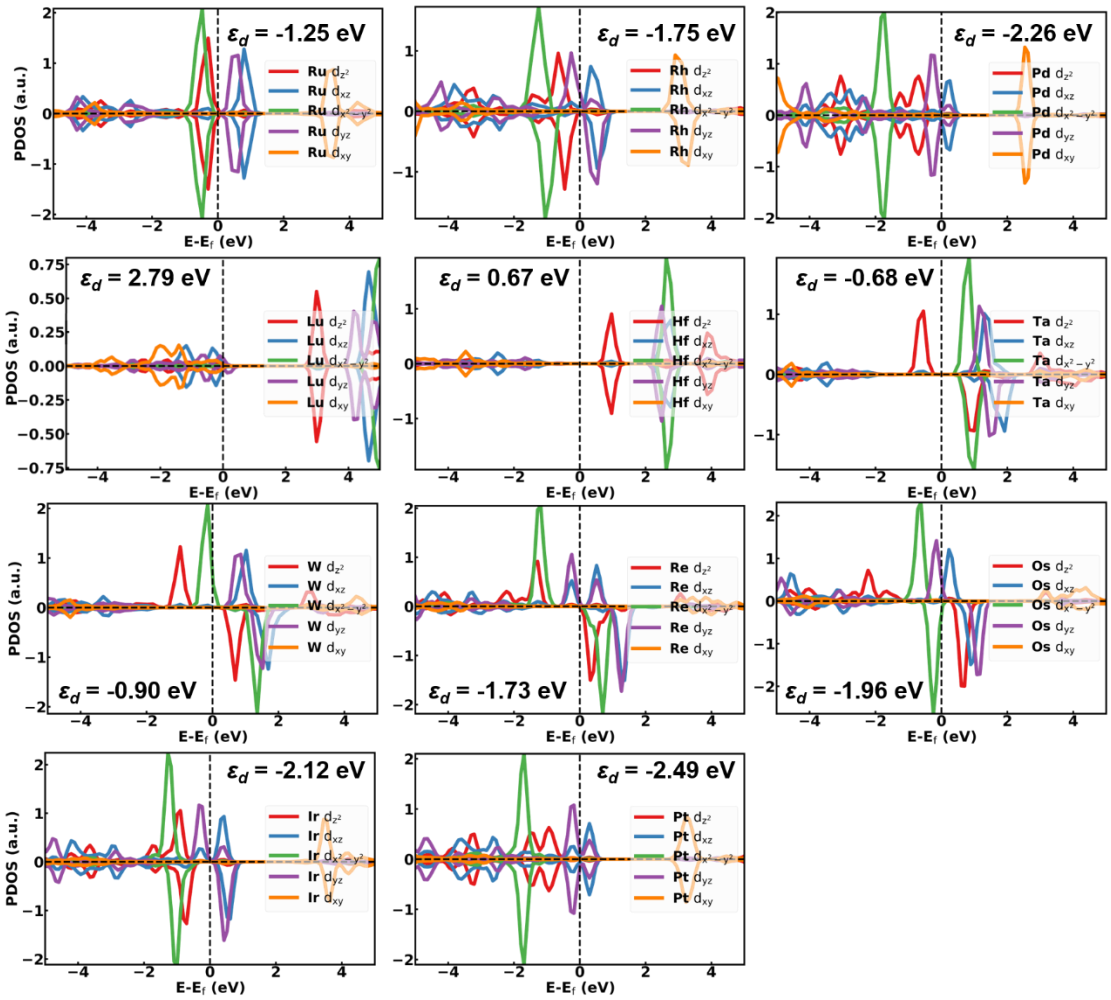

Fig. S7. Projected density of states (PDOS) of *d* orbitals and corresponding *d*-band centers for TM@BNNCs (TM = Ru, Rh, Pd, Lu, Hf, Ta, W, Re, Os, Ir, and Pt).

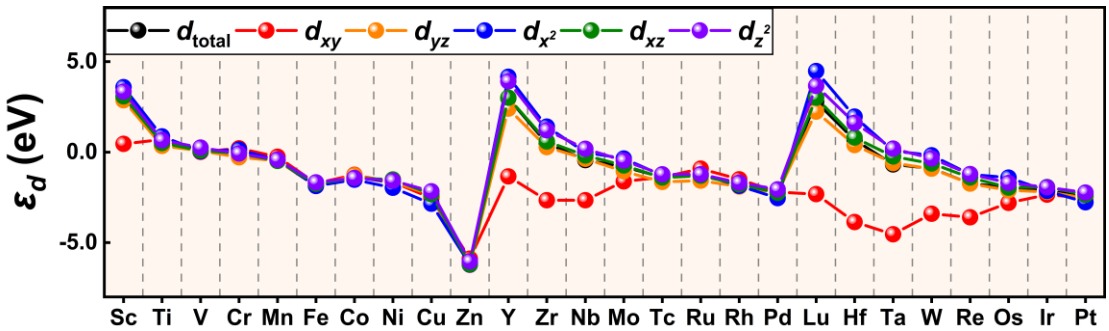

Fig. S8. *d*-band centers (ε_d) of *d* orbitals for TM@BNNCs (orbitals = d, d_{xy}, d_{yz}, d_x^2, d_{xz} and d_z^2).

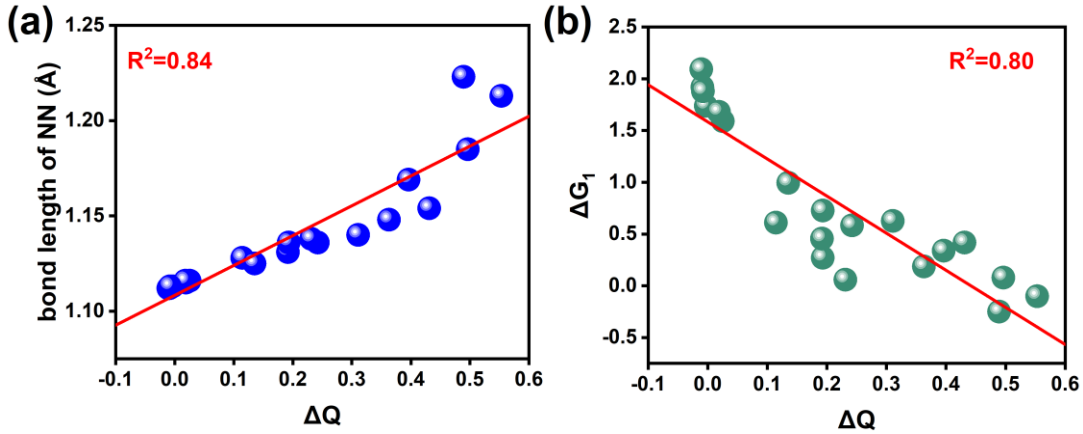

Fig. S9. The correlation of (a) ΔQ versus bond length of $*N_2$ and (b) ΔQ versus ΔG_1 on TM@BNNCs during various corresponding NRR pathways.

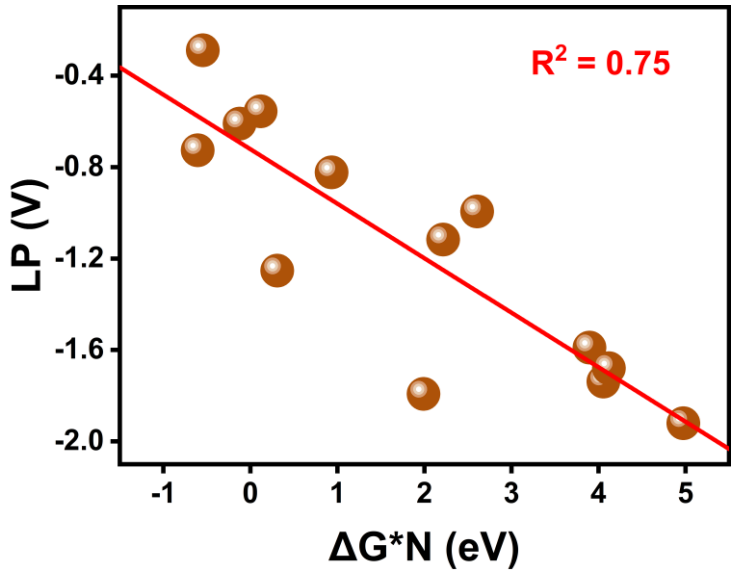

Fig. S10. The linear fit between LP and Δ*G**N = *G**N – *G**. The catalysts are TM@BNNCs that pass the screening.

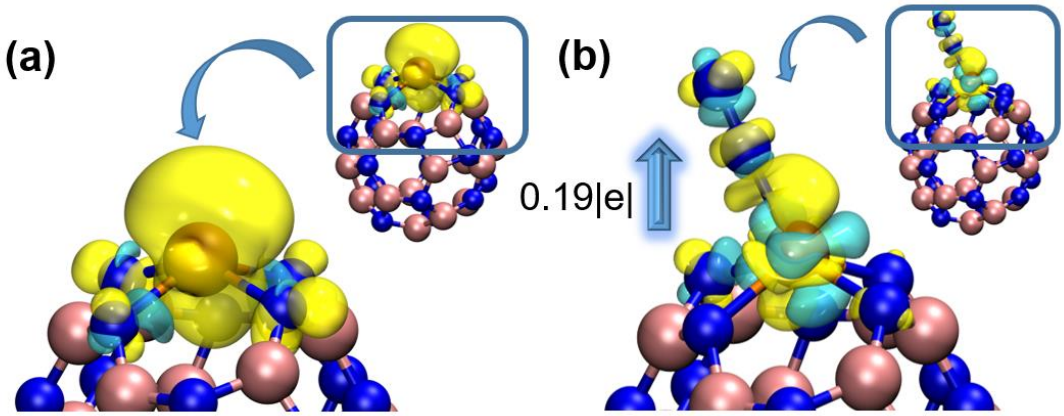

Fig. S11. (a) Magnetization distribution (spin density) and (b) charge difference (Charge density) with charge transfer from Os@BNNC to N_2 caused by adsorption of N_2.

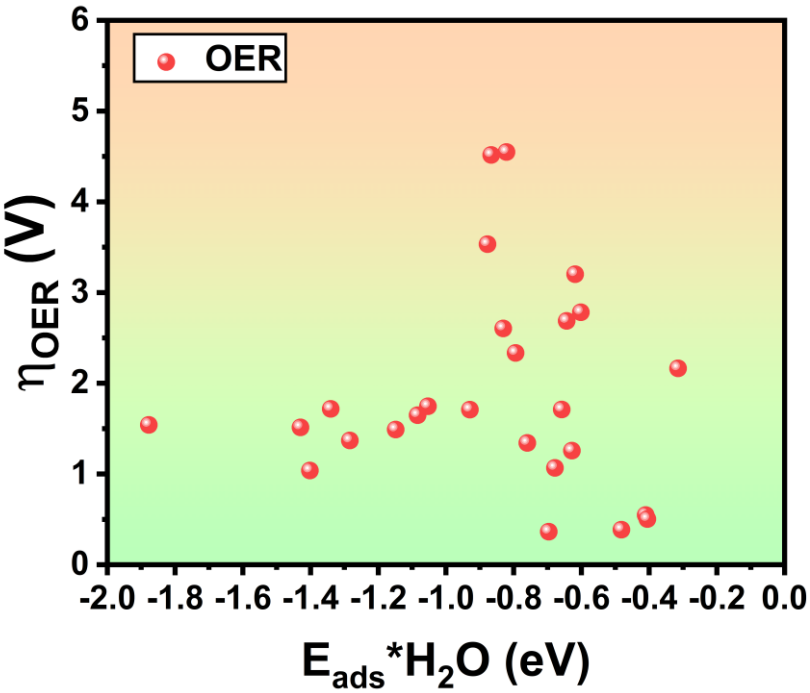

Fig. S12. The scatter plot of overpotential of OER with E_{ads}(*H_2O) for TM@BNNCs.

References

1. Y. Li, W. Nong, Z. H. Zeng and C. X. Wang, *Advanced Energy Materials*, 2022, **13**, 2203159.
2. Charles Kittel, *Introduction to Solid State Physics*, John Wiley & Sons, Inc., Hoboken, NJ, 2005.
3. A. A. Peterson, F. Abild-Pedersen, F. Studt, J. Rossmeisl and J. K. Nørskov, *Energy Environ. Sci.*, 2010, **3**, 1311.
4. R. Johnson, 2013.
5. W. Nong, S. H. Qin, F. Huang, H. K. Liang, Z. Yang, C. Z. Qi, Y. Li and C. X. Wang, *Carbon*, 2021, **182**, 297-306.
6. C. Choi, S. Back, N. Y. Kim, J. Lim, Y. H. Kim and Y. Jung, *Acs Catalysis*, 2018, **8**, 7517-7525.
7. T. T. Yang, S. B. Tang, X. Y. Li, E. Sharman, J. Jiang and Y. Luo, *Journal of Physical Chemistry C*, 2018, **122**, 25441-25446.
8. X. Guo and S. Huang, *Electrochimica Acta*, 2018, **284**, 392-399.
9. Y. Cao, Y. Gao, H. Zhou, X. Chen, H. Hu, S. Deng, X. Zhong, G. Zhuang and J. Wang, *Advanced Theory and Simulations*, 2018, **1**, 1800018.
10. X. Chen, X. Zhao, Z. Kong, W.-J. Ong and N. Li, *Journal of Materials Chemistry A*, 2018, **6**, 21941-21948.
11. C. Ling, X. Bai, Y. Ouyang, A. Du and J. Wang, *The Journal of Physical Chemistry C*, 2018, **122**, 16842-16847.
12. Z. Wang, Z. Yu and J. Zhao, *Phys Chem Chem Phys*, 2018, **20**, 12835-12844.
13. C. Y. Ling, Y. X. Ouyang, Q. Li, X. W. Bai, X. Mao, A. J. Du and J. L. Wang, *Small Methods*, 2019, **3**, 1800376.
14. Y. Yang, J. Liu, Z. Wei, S. Wang and J. Ma, *ChemCatChem*, 2019, **11**, 2821-2827.
15. H. Yin, S.-L. Li, L.-Y. Gan and P. Wang, *Journal of Materials Chemistry A*, 2019, **7**, 11908-11914.
16. Z. Chen, J. Zhao, C. R. Cabrera and Z. Chen, *Small Methods*, 2018, **3**, 1800368.
17. X. Liu, Y. Jiao, Y. Zheng, M. Jaroniec and S. Z. Qiao, *J Am Chem Soc*, 2019, **141**, 9664-9672.
18. C. Liu, Q. Li, J. Zhang, Y. Jin, D. R. MacFarlane and C. Sun, *Journal of Materials Chemistry A*, 2019, **7**, 4771-4776.
19. Z. W. Chen, J.-M. Yan and Q. Jiang, *Small Methods*, 2019, **3**, 1800291.
20. X. Zhang, A. Chen, Z. Zhang and Z. Zhou, *Journal of Materials Chemistry A*, 2018, **6**, 18599-18604.
21. L. M. Azofra, C. Sun, L. Cavallo and D. R. MacFarlane, *Chemistry*, 2017, **23**, 8275-8279.
22. J. Zheng, Y. Lyu, M. Qiao, J. P. Veder, R. D. Marco, J. Bradley, R. Wang, Y. Li, A. Huang, S. P. Jiang and S. Wang, *Angew Chem Int Ed Engl*, 2019, **58**, 18604-18609.
23. L. Shi, Q. Li, C. Ling, Y. Zhang, Y. Ouyang, X. Bai and J. Wang, *Journal of*

Materials Chemistry A, 2019, **7**, 4865-4871.
24. T. Yang, T. T. Song, J. Zhou, S. Wang, D. Chi, L. Shen, M. Yang and Y. P. Feng, *Nano Energy*, 2020, **68**, 104304.
25. S. Ji, Z. Wang and J. Zhao, *Journal of Materials Chemistry A*, 2019, **7**, 2392-2399.
26. Z. Geng, Y. Liu, X. Kong, P. Li, K. Li, Z. Liu, J. Du, M. Shu, R. Si and J. Zeng, *Adv. Mater.*, 2018, **30**, 1803498.
27. W. Gu, Y. Guo, Q. Li, Y. Tian and K. Chu, *ACS Appl Mater Interfaces*, 2020, **12**, 37258-37264.
28. K. Chu, Y.-p. Liu, Y.-h. Cheng and Q.-q. Li, *Journal of Materials Chemistry A*, 2020, **8**, 5200-5208.
29. Q. Li, Y. Guo, Y. Tian, W. Liu and K. Chu, *Journal of Materials Chemistry A*, 2020, **8**, 16195-16202.
30. K. Chu, Y.-h. Cheng, Q.-q. Li, Y.-p. Liu and Y. Tian, *Journal of Materials Chemistry A*, 2020, **8**, 5865-5873.
31. K. Chu, J. Wang, Y.-p. Liu, Q.-q. Li and Y.-l. Guo, *Journal of Materials Chemistry A*, 2020, **8**, 7117-7124.
32. J. Cao, N. Li and X. Zeng, *New Journal of Chemistry*, 2021, **45**, 6327-6335.
33. B. Huang, Y. Wu, B. Chen, Y. Qian, N. Zhou and N. Li, *Chinese Journal of Catalysis*, 2021, **42**, 1160-1167.
34. J. Zhao and Z. Chen, *J Am Chem Soc*, 2017, **139**, 12480-12487.
35. G. Centi and S. Perathoner, *Small*, 2021, **17**, 2007055.
36. W. Song, K. Xie, J. Wang, Y. Guo, C. He and L. Fu, *Phys Chem Chem Phys*, 2021, **23**, 10418-10428.
37. Y. Fu, T. Li, G. Zhou, J. Guo, Y. Ao, Y. Hu, J. Shen, L. Liu and X. Wu, *Nano Lett*, 2020, **20**, 4960-4967.
38. Y. R. Ying, K. Fan, X. Luo, J. L. Qiao and H. T. Huang, *Journal of Materials Chemistry A*, 2021, **9**, 16860-16867.
39. Z. Xue, X. Y. Zhang, J. Q. Qin and R. P. Liu, *Journal of Energy Chemistry*, 2021, **55**, 437-443.
40. X. Li, Z. Su, Z. Zhao, Q. Cai, Y. Li and J. Zhao, *J Colloid Interface Sci*, 2022, **607**, 1005-1013.
41. P. Y. Shan, X. Bai, Q. Jiang, Y. J. Chen, S. Lu, P. Song, Z. P. Jia, T. Y. Xiao, Y. Han, Y. Z. Wang, T. Liu, H. Cui, R. Feng, Q. Kang, Z. Y. Liang and H. K. Yuan, *Renewable Energy*, 2023, **203**, 445-454.
42. H. Jiang, J. Gu, X. Zheng, M. Liu, X. Qiu, L. Wang, W. Li, Z. Chen, X. Ji and J. Li, *Energy Environ. Sci.*, 2019, **12**, 322-333.
43. X. Zhang, Z. Yang, Z. Lu and W. Wang, *Carbon*, 2018, **130**, 112-119.
44. X. P. Sun, S. X. Sun, S. Q. Gu, Z. F. Liang, J. X. Zhang, Y. Q. Yang, Z. Deng, P. Wei, J. Peng, Y. Xu, C. Fang, Q. Li, J. T. Han, Z. Jiang and Y. H. Huang, *Nano Energy*, 2019, **61**, 245-250.
45. E. P. Wang, B. K. Zhang, J. Zhou and Z. M. Sun, *Appl. Surf. Sci.*, 2022, **604**, 154522.
46. J. Wan, C. Wang, Q. Tang, X. Gu and M. He, *RSC Adv*, 2019, **9**, 37467-37473.

47. S. Xu, M. Wang, G. Saranya, N. Chen, L. Zhang, Y. He, L. Wu, Y. Gong, Z. Yao, G. Wang, Z. Wang, S. Zhao, H. Tang, M. Chen and H. Gou, *Applied Catalysis B: Environmental*, 2020, **268**, 118385.
48. Y. Yu, J. Zhou and Z. Sun, *Advanced Functional Materials*, 2020, **30**, 2000570.
49. X. Bai, Q. Wang, G. Xu, Y. Ning, K. Huang, F. He, Z. J. Wu and J. Zhang, *Chemistry*, 2017, **23**, 16862-16870.
50. D. Kan, D. Wang, X. Zhang, R. Lian, J. Xu, G. Chen and Y. Wei, *Journal of Materials Chemistry A*, 2020, **8**, 3097-3108.
51. H. Xu, D. Cheng, D. Cao and X. C. Zeng, *Nat. Catal.*, 2018, **1**, 339-348.